

Instance-aware Dynamic Prompt Tuning for Pre-trained Point Cloud Models

Yaohua Zha¹, Jinpeng Wang¹, Tao Dai^{2*}, Bin Chen³, Zhi Wang¹, and Shu-Tao Xia^{1,4}

¹ Tsinghua Shenzhen International Graduate School, Tsinghua University

² College of Computer Science and Software Engineering, Shenzhen University

³ Harbin Institute of Technology, Shenzhen

⁴ Research Center of Artificial Intelligence, Peng Cheng Laboratory

Abstract

Recently, pre-trained point cloud models have found extensive applications in downstream tasks like object classification. However, these tasks often require full fine-tuning of models and lead to storage-intensive procedures, thus limiting the real applications of pre-trained models. Inspired by the great success of visual prompt tuning (VPT) in vision, we attempt to explore prompt tuning, which serves as an efficient alternative to full fine-tuning for large-scale models, to point cloud pre-trained models to reduce storage costs. However, it is non-trivial to apply the traditional static VPT to point clouds, owing to the distribution diversity of point cloud data. For instance, the scanned point clouds exhibit various types of missing or noisy points. To address this issue, we propose an Instance-aware Dynamic Prompt Tuning (IDPT) for point cloud pre-trained models, which utilizes a prompt module to perceive the semantic prior features of each instance. This semantic prior facilitates the learning of unique prompts for each instance, thus enabling downstream tasks to robustly adapt to pre-trained point cloud models. Notably, extensive experiments conducted on downstream tasks demonstrate that IDPT outperforms full fine-tuning in most tasks with a mere 7% of the trainable parameters, thus significantly reducing the storage pressure. Code is available at <https://github.com/zyh16143998882/IDPT>.

1. Introduction

With the rapid development of 3D scanning technology, point clouds, as irregular point sets that represent 3D geometry, have been widely used in various fields and tasks. Deep learning-based point cloud processing techniques [16, 25, 32, 34, 35, 45] have drawn considerable attention as they can directly process raw point cloud data

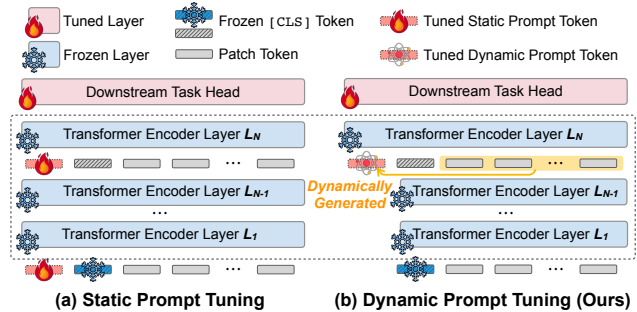


Figure 1. The pipeline of (a) the previous static prompt tuning in VPT [23] and (b) our dynamic prompt tuning. Unlike the static prompt tuning that is instance-agnostic, ours is adaptive to input by concatenating the instance-adaptive prompt generated by a prompt module into the last Transformer layer input.

while preserving its rich information. As a classic deep learning paradigm, fine-tuning the foundation model pre-trained [11, 27, 33, 51, 54] on massive raw point clouds in specific downstream tasks has achieved state-of-the-art performance. However, this approach is storage-intensive, as it requires storing and deploying a separate copy of the backbone parameters for each task.

Recently, prompt tuning has surpassed fine-tuning in multiple downstream tasks in the language and image domains, significantly reducing storage requirements by fixing the parameters of a pre-trained model and introducing a small amount of task-specific learnable parameters into the input space. Although some works [22, 21, 46, 53] attempt to introduce prompt into point cloud processing, they all rely on pre-trained image models (e.g. CLIP [38], ViT [12], etc.). To date, less research has been denoted to prompt tuning in point cloud pre-trained models.

Inspired by the success of visual prompt tuning (VPT) [23]), it is natural to adopt the traditional static prompt-tuning in VPT to point clouds, as shown in Figure 1

(a), whereby we introduced a few learnable parameters as prompts to each layer input of a pre-trained point cloud Transformer. During the fine-tuning phase in downstream tasks, we froze the pre-trained Transformer parameters and updated only the downstream task head and prompt parameters. Although such a strategy performs well on synthetic datasets (e.g. ModelNet40 [47]), it causes significant performance degradation on real scanned point cloud datasets (e.g. ScanObjectNN [41]). Thus, static prompt tuning is not suitable for real point clouds, where point clouds with different types of missing or noisy points belong to different distributions. These observations motivate us to design a universal prompt tuning strategy for both synthetic and real point clouds.

To address this issue, we proposed an Instance-aware Dynamic Prompt Tuning (IDPT) for point cloud pre-trained models, which is an instance-adaptive prompt tuning. As shown in Figure 1 (b), IDPT uses a prompt module to perceive the semantic prior of each instance and learns unique prompts for each point cloud via this semantic prior. The instance-aware dynamic prompt enables us to pair inputs with different distribution domains into the same domain, thereby enhancing the robustness of the Transformer [43] backbone. Our IDPT only concatenates prompts in the input of the last Transformer layer, which allows for a more accurate representation of the semantic prior to each point cloud. This semantic prior facilitates the learning of unique prompts for each instance, thus enabling downstream tasks to robustly adapt to pre-trained point cloud models.

The main contributions can be summarized as follows:

- We investigate static prompt tuning in vision, which is instance-agnostic, to point cloud pre-trained models, and have found that the static prompt tuning cannot work well in real point clouds due to the distribution diversity. To the best of our knowledge, this is the first exploration of utilizing prompt tuning in point cloud pre-trained models.
- We propose an Instance-aware Dynamic Prompt Tuning (IDPT) to produce a universal prompt for both synthetic and real point clouds, which is adaptive to instance input. Specifically, IDPT learns a unique prompt from the semantic prior of each point cloud to cope with the distribution diversity issues existing in point cloud data.
- Extensive experiments on a variety of downstream tasks have shown that our IDPT reaches state-of-the-art performance in most tasks, and particularly, our IDPT significantly reduces the storage cost of pre-trained models by using only 7% of the trainable parameters of full fine-tuning.

2. Related Work

2.1. Point Cloud Pre-training Model

Recently, studies on pre-trained foundational models for 3D point clouds have achieved remarkable success. These approaches first apply a pretext task to pre-train the foundational model to learn the latent semantic information of the point cloud and then fine-tune the model weights for the target task to achieve higher performance. Existing pre-train pretext tasks can be divided into discriminative tasks [4, 9, 14, 48] and generative tasks [3, 11, 19, 26, 27, 33, 51, 54]. The discriminative approach distinguishes different views of the same point cloud instance from other instances, PointContrast [49] and CrossPoint [1] explore the use of contrast learning of intra-domain and cross-domain features to obtain rich self-supervised information. Generation methods typically rely on an autoencoder to learn the latent features of the data by reconstructing the original input. Point-BERT [51], Point-MAE [33] and PointM2AE [54], based on masked autoencoders, have been very successful. Additionally, Point-DAE [54] explores a more general denoising autoencoder for point cloud learning by investigating more types of corruption beyond masking. ACT [11] achieves a significant improvement on real scanned point clouds by using pre-trained language models and image models as cross-modal teachers to guide the learning of 3D self-supervised networks. However, the above methods all utilize full fine-tuning to adapt pre-trained models to various downstream tasks. Our work further explores how to reduce parameter storage in downstream tasks by utilizing prompt tuning, building upon the aforementioned approach.

2.2. Prompt Learning in Computer Vision

Prompt tuning involves adding specific prompt information to the input of a pre-trained model and adjusting downstream tasks to fit the pre-trained model. This is achieved by fixing the pre-trained model parameters and fine-tuning the prompt. It was first proposed in the language model [7, 13, 24, 28, 29, 30] and gained popularity in the image model [38, 39, 40, 56, 55] later due to its flexibility and high performance. CLIP [38] uses fixed class-specific text labels as prompts for prediction. Later, CoOp [56] learns class-specific continuous prompts, and CoCoOp [55] builds upon CoOp by introducing a lightweight network to learn dynamic prompts for each instance. VPT [23] first introduces the continuous prompt tuning framework into image pre-trained models inspired by P-Tuning [29]. Additionally, P2P [46] achieved the first application of prompts in point clouds by learning color information in the input space of point cloud rendering images as prompts for the 2D backbone network. PointCLIP [53] and CLIP2Point [21] project the point cloud as a depth map and then use the pre-trained CLIP [38] to understand the point cloud. However, all the

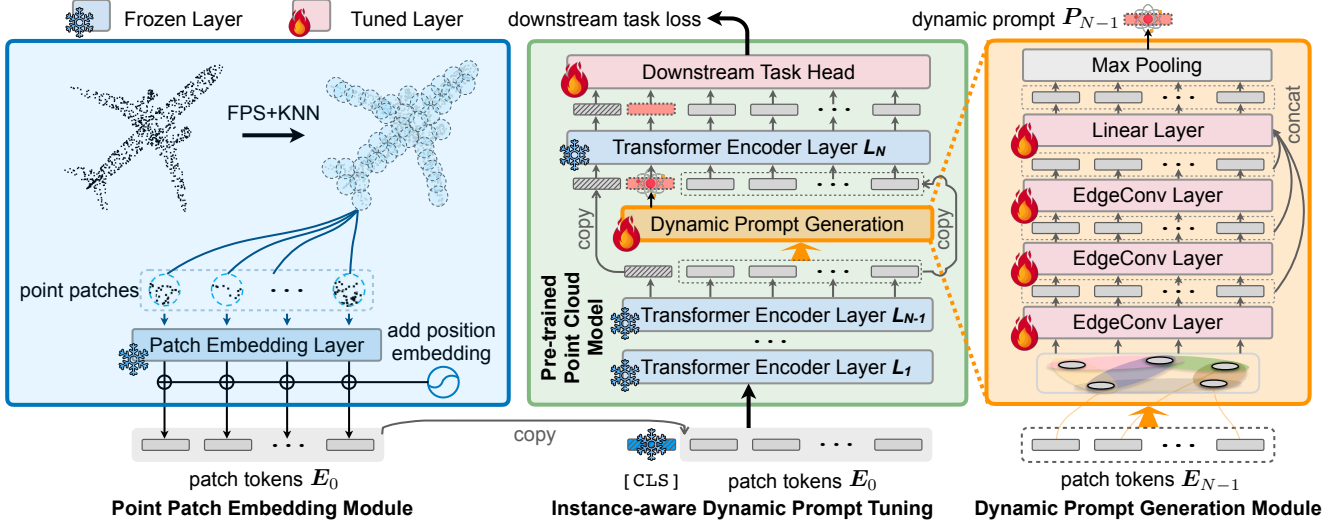


Figure 2. Overall pipeline of Instance-aware Dynamic Prompt Tuning (IDPT) for pre-trained point cloud models, which only updates the parameters of the dynamic prompt generation module and downstream task head during a downstream tuning task. To capture various sub-modes existing in the real-world data and enhance the robustness against noises (e.g., with different types of missing or noisy points), we design a dynamic prompt generation module with graph convolution [45] layers to aggregate multi-scale contextual features and dynamically generate instance-adaptive prompt. Empirically, inserting the dynamic prompt before the last transformer layer yields promising performance and enjoys decent efficiency at the same time.

above work relies on pre-trained image models. Our work discusses the tuning of pre-trained point cloud models with appropriate prompting mechanisms.

3. Methodology

In this section, we first introduce the tuning pipeline for a pre-trained point cloud model (§ 3.1). Next, we present the empirical observation of static prompt tuning (e.g. VPT [23]) and discuss its weaknesses (§ 3.2) that highlight our motivations. At last, we describe our Instance-aware Dynamic Prompt Tuning strategy in detail (§ 3.3).

3.1. Preliminaries

When fine-tuning a pre-trained point cloud model (e.g. Point-MAE [33]), a point cloud $\mathbf{X} \in \mathbb{R}^{M \times 3}$ with M points is first divided into m point patches $\mathbf{X}' \in \mathbb{R}^{m \times k \times 3}$ via Farthest Point Sampling (FPS) and K-Nearest Neighborhood (KNN) algorithms, where each patch has k local points. Then, all point patches will be embedded into a series of input tokens $\mathbf{E}_0 \in \mathbb{R}^{m \times d}$ with positional encoding via a point patch embedding module. Next, we insert a classification token (i.e., [CLS]) \mathbf{c}_0 at the head of the patch embeddings and forward the token embeddings to the pre-trained model. Specifically, the forward process of each transformer layer is defined as

$$[\mathbf{c}_i; \mathbf{E}_i] = f_i([\mathbf{c}_{i-1}; \mathbf{E}_{i-1}]), \quad i = 1, 2, \dots, N, \quad (1)$$

where f_i denotes the i -th transformer encoder layer. N is the total transformer layer number of the pre-trained back-

bone. Finally, the model makes predictions by building a task-specific head g_h upon the output of the pre-trained backbone:

$$\mathbf{y} = g_h([\mathbf{c}_N; \mathbf{E}_N]). \quad (2)$$

All the parameters of $\{f_i\}_{i=1}^N$ and g_h will be updated in a downstream tuning task, which burdens the storage cost for per-task model weights.

Recently, prompt [56, 23] has shown to be effective for parameter-efficient tuning. The basic idea of prompt tuning is to insert a few learnable prompt tokens into the input token sequence, i.e., we modify Eq.(1) and Eq.(2) by

$$[\mathbf{c}_i; \mathbf{P}_i; \mathbf{E}_i] = f_i([\mathbf{c}_{i-1}; \mathbf{P}_{i-1}; \mathbf{E}_{i-1}]), \quad i = 1, 2, \dots, N, \quad (3)$$

$$\mathbf{y} = g_h([\mathbf{c}_N; \mathbf{P}_N; \mathbf{E}_N]), \quad (4)$$

where \mathbf{P}_i is the inserted prompt tokens at the i -th layer. During the tuning process, we freeze the parameters of $\{f_i\}_{i=1}^N$ and only update prompt $\{\mathbf{P}_i\}_{i=1}^N$ and task-specific head g_h , which can largely reduce per-task storage cost.

3.2. Observation and Discussion

Inspired by the success of Visual Prompt Tuning (VPT) [23], it is natural to extend such a prompting tuning strategy to point clouds, as shown in Figure 1(a). As the prompt tokens are instance-independent and shared by all samples during downstream tuning, we term this kind of strategy *static prompt tuning*. Our empirical study showed

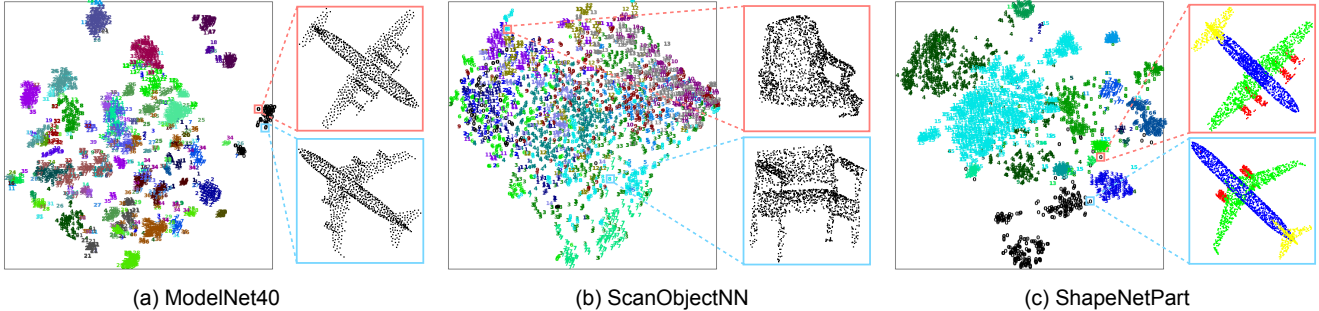


Figure 3. The t-SNE [42] visualization of the point cloud features extracted from with the Point-MAE [33] on three datasets: (a) ModelNet40, (b) ScanObjectNN, and (c) ShapeNetPart. Different from synthetic datasets (*e.g.* ModelNet40 and ShapeNetPart) with clean and compact cluster structures, in real-world datasets (*e.g.* ScanObjectNN), instances within the same category can present various sub-modes (*i.e.* sub-clusters scattered in the embedding space) because real-world point clouds contain varying types of missing or noisy points.

Tuning Strategy	#TP (M)	ModelNet40	ScanObjectNN		
			OBJ_BG	OBJ_ONLY	PB_T50_RS
Full Fine-tuning	22.10	93.8	92.12	92.01	88.41
Only Head Tuning	0.27	93.2	87.40	87.13	80.33
VPT-Shallow [23]	0.28	93.4	87.61	89.04	80.99
VPT-Deep [23]	0.36	93.6	89.98	90.19	83.96

Table 1. Classification accuracy (%) for different tuning strategies is reported. All experiments were conducted based on a pre-trained Point-MAE [33] model, and a simple rotation augmentation in ACT [11] was employed on the ScanObjectNN [41] dataset. ‘#TP’ denotes the number of trainable parameters.

that although VPT improves downstream performance compared with tuning the task head only, it underperforms fully fine-tuning by considerable margins. In particular, Table 1 presents the results of classification on several benchmark datasets. We can learn that static prompt tuning significantly reduces the number of trainable parameters (*i.e.*, about 1% to 2% of backbone parameters) compared with fully fine-tuning. In terms of accuracy, although VPT-Deep performs well on synthetic datasets (*e.g.* ModelNet40 [47]), it presents significant performance degradation on real scanned point cloud datasets. For example, on the PB_T50_RS variant of ScanObjectNN [41] dataset, fully fine-tuning outperforms VPT-Deep by 4.5% accuracy.

Here we briefly discuss why static prompt tuning performs well on synthetic datasets but poorly on real scanned datasets. We adopt a perspective from Domain Adaptation (DA) [2, 5, 6, 17] and consider the transferring from pre-trained models to downstream tasks. Our goal is to bridge the source and target domains with different distributions so as to enhance the prediction robustness of the pre-trained model. By definition, the source domain $p_s(\mathbf{x}_s)$ refers to the distribution of pre-training data, and the target domain $p_t(\mathbf{x}_t)$ refers to the distribution of downstream task data. Empirically, we found that

$$p_t(\mathbf{x}_t) \neq p_s(\mathbf{x}_s), \quad (5)$$

while we ask for a robust model such that

$$p_t(\mathbf{y}_t|\mathbf{x}_t) = p_s(\mathbf{y}_s|\mathbf{x}_s), \quad (6)$$

where \mathbf{x} denotes the input and \mathbf{y} denotes the output. Therefore, the goal of domain adaptation is to find a transformation $\Phi(\cdot)$, such that

$$p_t(\Phi(\mathbf{x}_t)) = p_s(\Phi(\mathbf{x}_s)). \quad (7)$$

Both fine-tuning and prompt tuning can be regarded as approaches to approximate the transformation $\Phi(\cdot)$. Fine-tuning adjusts all parameters of the pre-trained model to fit Φ , whereas prompt tuning introduces additional prompt parameters to fit Φ . From Table 1, we can learn that full fine-tuning achieves satisfactory performance by fitting all model parameters. In contrast, the static prompt shows inflexibility in mitigating the domain gap, suffering from the noises in the target domain.

We also provide an intuitive analysis of such a phenomenon. Specifically, Figure 3 shows the t-SNE [42] visualization of point cloud features extracted with Point-MAE [33] on the test sets of three datasets: (a) ModelNet40 [47], (b) ScanObjectNN [41], and (c) ShapeNetPart [50]). It reflects the downstream task data distribution (*i.e.*, target domain) to some degree. As shown in the figure, on synthetic datasets like ModelNet40 and ShapeNetPart, instances from the same class tend to distribute in relatively clear and tight clusters. Quite differently on the real scanned dataset ScanObjectNN, instances from the same class scatter to many sub-clusters in the feature space, indicating the mixing of various sub-distributions corresponding to different sub-modes. Our intuition is that synthetic datasets like ModelNet40 and ShapeNetPart contain complete, uniform, and relatively clean point clouds, such as the airplanes shown in Figures 3(a) and 3(c). In contrast, ScanObjectNN consists of real scanned point clouds with varying types of missing or noisy points, making up different sub-modes within the same class. For example, Figure 3(b) shows two

kinds of chairs: one is mostly missing, while the other is more complete. As static prompt tuning fails to capture various sub-modes in real-world data distribution, it highlights the necessity of an adaptive or dynamic prompting strategy.

3.3. Instance-aware Dynamic Prompt Tuning

To address the aforementioned issues of static prompt tuning, we propose **Instance-aware Dynamic Prompt Tuning (IDPT)**. Figure 2 shows the pipeline of IDPT.

3.3.1 Dynamic Prompt Generation Module

To capture various sub-modes existing in the real-world data and enhance the robustness against noises (*e.g.*, with different types of missing or noisy points), we utilized EdgeConv [45] at the patch level to perceive local point cloud shapes at a larger scale. Specifically, as shown in Figure 2, point patch tokens E_{N-1} are processed by three EdgeConvs to generate three patch features at different scales. Then, the multi-scale patch features are concatenated and fed into a linear layer, followed by max pooling to generate an instance-aware dynamic prompt P_{N-1} :

$$P_{N-1} = \varphi_P(E_{N-1}). \quad (8)$$

$\varphi_P(\cdot)$ denotes the dynamic prompt generation module.

Next, we forward P_{N-1} accompany with E_{N-1} to the last transformer layer f_N :

$$[c_N; P_N; E_N] = f_N([c_{N-1}; P_{N-1}; E_{N-1}]). \quad (9)$$

Finally, we concatenate [CLS] token c_N , prompt token P_N , and patch tokens E_N together before feeding them into a task head. The final prediction is made by:

$$y = g_h([c_N; P_N; E_N]). \quad (10)$$

3.3.2 Prompt Insert Position

Perceiving various sub-modes in real-world point cloud data relies on high-level semantic information. As higher (or deeper) transformer layers grasp global semantic information (*e.g.* density, shape, or categorical information) better, IDPT prefers to insert prompts at deeper transformer layers to ensure an accurate perception of point cloud semantics. In particular, we found that inserting the dynamic prompt before the last transformer layer yields robust performance and also enjoys decent efficiency. We provide detailed quantitative analysis in § 4.3.4.

4. Experiments

We evaluated the performance of our proposed Instance-aware Dynamic Prompt Tuning (IDPT) on classification, few-shot learning, and segmentation tasks. Then, we discussed the benefits of our tuning strategy and architecture in

the ablation study section. We used three classic pre-trained models (Point-Bert [51], Point-MAE [33], and ACT [11]) as our baseline. Notably, our IDPT is a universal paradigm that can be applied to any pre-trained point cloud model.

4.1. Experiment Settings

To ensure a fair comparison, we have used the same experimental settings as the default fine-tuning method for each baseline. This involves freezing the weights of the pre-trained point cloud model and only updating the parameters of the Prompt Model and Head during downstream task training. All experiments were conducted on a single GeForce RTX 3090 24GB. We have explored the performance of the simple rotation augmentation from ACT [11] on the ScanObjectNN [41] dataset, which is denoted as † in our table. For all other experiments, default data augmentation was used. We provide segmentation results and additional ablation experimental results in the Appendix due to space limitations.

4.2. Prompt Tuning on Downstream Tasks

4.2.1 Object Classification on Real-World Dataset

In the study of point cloud pre-training models, it is common practice to conduct pre-training on the ShapeNet [8] dataset, which typically only contains clean point clouds and assumes that all point clouds are identically distributed. However, in reality, point clouds often suffer from issues such as noise and missing points, resulting in a diverse distribution. We first assess our IDPT performance on the ScanObjectNN [41] dataset, which consists of about 15K point cloud samples by 15 categories. These objects are scanned indoor scene data, which are usually cluttered with background and occluded by other objects.

We conducted experiments on three variants of ScanObjectNN [41] (OBJ-BG, OBJ-ONLY, and PB-T50-RS). The results are shown in Table 2, † indicates that the pre-trained model used simple rotational augmentation of ACT during fine-tuning or prompt tuning, and without † indicates the default augmentation method. We observed that: (i) We achieved state-of-the-art (SOTA) performance with IDPT on Point-MAE†. In comparison to the current state-of-the-art method ACT, we have achieved gains of 0.34%, 1.21%, and 0.3% respectively in the three variants of ScanObjectNN, while utilizing only 7% of its trainable parameters. (ii) Our IDPT outperforms full fine-tuning in most cases with fewer trainable parameters. These results demonstrate the excellent performance of our method on real scanned point clouds with various data distributions. We believe this is due to the introduction of a semantic prior of real point cloud data on the one hand, and fewer trainable parameters to mitigate overfitting on the other.

Method	#TP (M)	OBJ_BG(†)	OBJ_ONLY(†)	PB_T50_RS(†)
<i>Supervised Learning Only</i>				
PointNet [34]	3.5	73.3	79.2	68.0
PointNet++ [35]	1.5	82.3	84.3	77.9
DGCNN [45]	1.8	82.8	86.2	78.1
PointCNN [25]	0.6	86.1	85.5	78.5
BGA-DGCNN [41]	1.8	-	-	79.7
BGA-PN++ [41]	1.5	-	-	80.2
DRNet [36]	-	-	-	80.3
GBNet [37]	8.8	-	-	80.5
SimpleView [15]	-	-	-	80.8
PRANet [10]	2.3	-	-	81.0
MVTN [18]	-	-	-	82.8
PointMLP [32]	-	-	-	85.7
<i>with Self-Supervised Representation Learning</i>				
Transformer [51]	22.1	79.86	80.55	77.24
OcCo [51]	22.1	84.85	85.54	78.79
Point-BERT [51]	22.1	87.43	88.12	83.07
MaskPoint [27]	22.1	89.70	89.30	84.60
Point-MAE [33]	22.1	90.02	88.29	85.18
Point-M2AE [33]	-	91.22	88.81	86.43
ACT [†] [11]	22.1	93.29	91.91	88.21
Point-MAE [†] [33]	22.1	92.94	92.08	88.41
Point-BERT w/ IDPT	1.7	88.12 († 0.69)	88.30 († 0.18)	83.69 († 0.62)
Point-MAE w/ IDPT	1.7	91.22 († 1.20)	90.02 († 1.73)	84.94 (↓ 0.24)
ACT[†] w/ IDPT	1.7	93.12 (↓ 0.17)	92.26 († 0.35)	87.65 (↓ 0.56)
Point-MAE[†] w/ IDPT	1.7	93.63 († 0.69)	93.12 († 1.04)	88.51 († 0.10)

Table 2. Classification results on three variants of ScanObjectNN dataset, and we report the number of trainable parameters (#TP) and classification accuracy(%). † indicates that the pre-trained model used simple rotational augmentation of ACT during fine-tuning or prompt tuning. We achieve state-of-the-art performance with IDPT on Point-MAE[†] and our IDPT outperforms full fine-tuning in most cases with fewer trainable parameters.

4.2.2 Object Classification on Synthetic Dataset

We evaluate our pre-trained model on the ModelNet40 [47] dataset for object classification. ModelNet40 [47] includes 12,311 clean 3D CAD models for 40 categories. Each point cloud is complete, uniform, and noise-free, and all point clouds in the dataset are independently and identically distributed. We follow standard protocols to split ModelNet40 into 9843 instances for the training set and 2468 for the testing set. Standard random scaling and random translation are applied for data augmentation during training. For fair comparisons, we also use the standard voting method [31] during testing.

As shown in Table 3, Point-MAE with IDPT achieves state-of-the-art performance with an accuracy of 94.4%. This represents a 0.6% improvement compared to fine-tuning. Additionally, other pre-trained models with IDPT, such as Point-BERT and ACT, demonstrate certain improvements compared to full fine-tuning. These results suggest that the incorporation of semantic priors of each instance can yield significant improvements, even when the downstream task dataset is identically distributed.

4.2.3 Few-shot Learning

We conducted few-shot learning experiments on ModelNet40, using the n-way, m-shot setting, following previ-

Method	ST?	#TP (M)	Data Type	Accuracy (%)
<i>Supervised Learning Only</i>				
PointNet [34]	-	3.5	1k Points	89.2
PointNet++ [35]	-	1.5	1k Points	90.7
DGCNN [45]	-	1.8	1k Points	92.9
PCT [16]	N	2.9	1k Points	93.2
PVT [52]	N	-	1k Points	93.6
PointTransformer [52]	N	-	1k Points	93.7
MVTN [18]	-	11.2	12 Images	93.8
SimpleView [15]	-	-	6 Images	93.9
PointMLP [46]	-	14.9	1k Points	94.5
<i>with Self-Supervised Representation Learning</i>				
Transformer [51]	Y	22.1	1k Points	91.4
OcCo [51]	Y	22.1	1k Points	92.1
EPCL [22]	-	-	1k Points	92.9
Point-BERT [51]	Y	22.1	1k Points	93.2
ACT [11]	Y	22.1	1k Points	93.7
Point-MAE [33]	Y	22.1	1k Points	93.8
MaskPoint [27]	Y	22.1	1k Points	93.8
Point-M2AE [54]	N	-	1k Points	94.0
CLIP2Point [21]	-	-	10 Images	94.0
P2P [46]	-	1.2	1 Images	94.0
Point-BERT w/ IDPT	Y	1.7	1k Points	93.4 († 0.2)
ACT w/ IDPT	Y	1.7	1k Points	94.0 († 0.3)
Point-MAE w/ IDPT	Y	1.7	1k Points	94.4 († 0.6)

Table 3. Classification results on ModelNet40 [47] dataset. ‘ST’ indicates whether the backbone is a standard Transformer [43] without any special design or inductive bias. ‘1k Points’ indicates that the input data is 1k points and ‘n Images’ indicates that the input data is n images. Our IDPT outperforms full fine-tuning in each baseline with fewer trainable parameters.

	5-way		10-way	
	10-shot	20-shot	10-shot	20-shot
DGCNN-OcCo [44]	90.6±2.8	92.5±1.9	82.9±1.3	86.5±2.2
Transformer-OcCo [51]	94.0±3.6	95.9±2.3	89.4±5.1	92.4±4.6
Point-BERT [51]	94.6±3.1	96.3±2.7	91.0±5.4	92.7±5.1
MaskPoint [27]	95.0±3.7	97.2±1.7	91.4±4.0	93.4±3.5
EPCL [22]	95.1±2.7	97.3±1.6	91.1±4.2	93.5±3.8
Point-MAE [54]	96.3±2.5	97.8±1.8	92.6±4.1	95.0±3.0
Point-M2AE [33]	96.8±1.8	98.3±1.4	92.3±4.5	95.0±3.0
ACT [11]	96.8±2.3	98.0±1.4	93.3±4.0	95.6±2.8
Point-BERT w/ IDPT	96.0±1.7 (†)	97.2±2.6 (†)	91.9±4.4 (†)	93.6±3.5 (†)
Point-MAE w/ IDPT	97.3±2.1 (†)	97.9±1.1 (†)	92.8±4.1 (†)	95.4±2.9 (†)
ACT w/ IDPT	96.7±2.5 (↓)	98.2±0.9 (†)	92.4±4.5 (↓)	95.5±3.0 (↓)

Table 4. Few-shot classification performance on ModelNet40. We report the average classification accuracy (%) with the standard deviation (%) of 10 independent experiments. Our IDPT achieved performance gains in most cases compared to full fine-tuning in few-shot learning.

ous works [33, 51, 54]. The results for the settings of $n \in 5, 10$ and $m \in 10, 20$ are presented in Table 4. Our IDPT achieved performance gains in most cases compared to full fine-tuning, demonstrating its effectiveness in few-shot learning as well.

4.3. Ablation study

To investigate the architecture design and tuning settings of our proposed strategy, we conducted extensive ablation studies on classification tasks in 2 variants of ScanOb-

Index	Model	VPT	IDPT	Adapter	Tr. Param.	OBJ_BG	OBJ_ONLY
A (Baseline)	Fixed	✗	✗	✗	0.27	87.40	87.13
B (VPT-Shallow)	Fixed	Shallow	✗	✗	0.28	87.61	89.04
C (VPT-Deep)	Fixed	Deep	✗	✗	0.36	89.98	90.19
D (Adapter)	Fixed	✗	✗	✓	2.04	88.93	89.90
E (IDPT)	Fixed	✗	✓	✗	1.70	92.48	92.19
F (Fine-tuning)	Trainable	✗	✗	✗	22.10	92.12	92.01

Table 5. Influence of different tuning strategies. Our IDPT tuning strategy achieved the best performance and efficiency compared to other tuning strategies.

Prompt Strategy	Trainable Parameters Type	Tr. Param.	OBJ_BG	OBJ_ONLY
w/o prompt	Head	0.27	87.40	87.13
VPT-Deep	10 prompts + Head	0.36	89.98	90.19
VPT-Deep	28 prompts + Head	0.52	90.02	90.53
VPT-Deep	156 prompts + Head	1.70	90.19	90.53
IDPT	PM (1-layer MLP) + Head	0.52	91.43	90.98
IDPT	PM (3-layer MLPs) + Head	1.49	91.64	91.34
IDPT	PM (1 EdgeConv) + Head	0.81	91.77	91.67
IDPT	PM (2 EdgeConv) + Head	1.25	91.95	91.67
IDPT	PM (3 EdgeConv) + Head	1.70	92.48	92.19
IDPT	PM (1 Transformer layer) + Head	2.14	92.03	91.22

Table 6. Effect of the Number of Trainable Parameters and PM Structure.

jectNN [41] (OBJ_BG and OBJ_ONLY), and we report the average results of 10 repeated experiments.

4.3.1 Advantages of IDPT over Other Tuning strategies

In order to demonstrate the superiority of our proposed instance-aware dynamic prompt tuning over other tuning strategies (fine-tuning, VPT [23], and Adapter [20]), we conducted extensive ablation studies as shown in Table 5. The specific tuning strategies used are as follows: (A) Baseline (we fixed the pre-trained model and only tuned the Head), (B) VPT-Shallow [23], (C) VPT-Deep [23], (D) Adapter [20], (E) our IDPT, and (F) Fine-tuning.

Our IDPT tuning strategy has outperformed other tuning strategies by achieving the highest level of performance, while utilizing fewer trainable parameters. When compared to the baseline without prompt, we observed a 5.08% and 5.06% improvement on the two variants of ScanObjectNN, respectively. Our strategy also significantly outperformed traditional static prompt and the classic Adapter. Additionally, our method demonstrated a significant improvement over fine-tuning, as it greatly reduced the number of trainable parameters while still improving performance. Overall, these experiments clearly demonstrate that our IDPT tuning strategy is highly effective.

4.3.2 The Effect of the Number of Trainable Parameters and PM Structure

We conducted experiments with varying numbers of trainable parameters to evaluate the effectiveness of our models. In VPT-Deep, we adjusted the trainable parameters by controlling the number of prompts in each layer input.

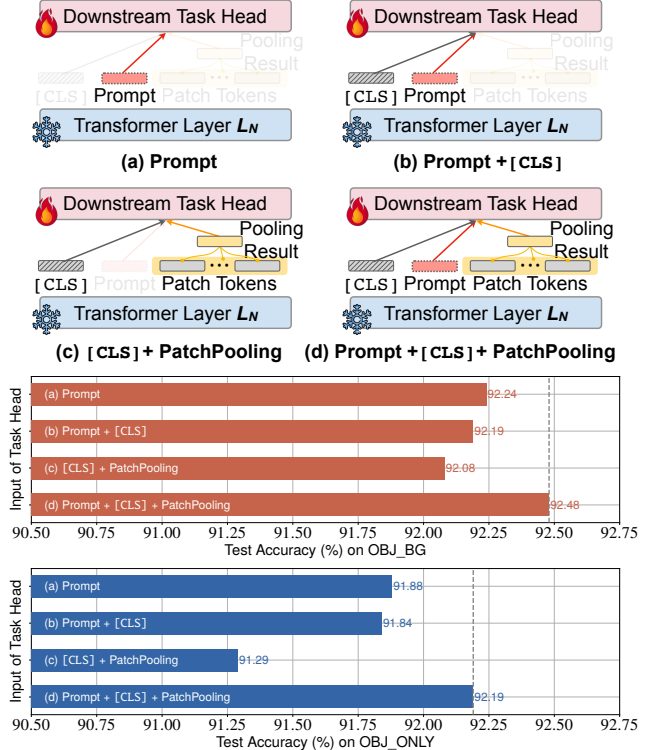


Figure 4. The effect of different Head inputs.

Meanwhile, in IDPT, we experimented with various network structures, including MLP, graph convolution (EdgeConv), and Transformer layers. Our experimental results, as shown in Table 6, demonstrate the following: (i) Using a single-layer MLP in IDPT resulted in significant improvements of 4.03% and 3.85% in OBJ_BG and OBJ_ONLY, respectively, when compared to the baseline without prompts. These results suggest that introducing semantic priors from the downstream task data can be highly effective. (ii) Increasing the number of parameters in VPT resulted in only limited performance improvements. It shows that merely increasing the number of parameters without introducing a semantic prior has limited performance improvement. (iii) For IDPT, EdgeConv proved to be an effective prompt module. Compared to MLP and Transformer, EdgeConv focuses more on local neighborhood information, allowing it to better perceive the specific shape of the point cloud and provide a better representation for downstream data semantic priors.

4.3.3 The Effect of Head inputs

We conducted an investigation on the impact of the downstream task head’s input features, which include the prompt token, the CLS token, and the max pooling of point patch tokens. The results are shown in Figure 4. We found that the highest performance was achieved when all three features were included (d): prompt token, CLS, and point patch to-

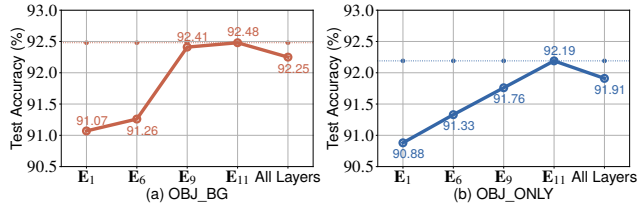


Figure 5. The effect of prompt insert position. E_i means to insert our dynamic prompt into the input of i -th layer of the pre-trained Transformer. 'All Layers' means to insert our dynamic prompt in each layer of the Transformer using a prompt module with shared parameters.

kens. When using only the dynamic prompt token (b), the performance was still strong and only second to the previous case. However, removing our prompt token (c) resulted in a slight decline in performance. These results indicate that the dynamic prompt token plays a critical role in guiding the downstream task fitting, as it contains specific and semantic information about the task data.

Although omitting the prompt feature in the head results in a performance decline, there is still a significant improvement when compared to traditional static prompts, as shown in Table 6. This suggests that our dynamic prompt is effective in aligning with different distributional data.

4.3.4 Effect of Prompt Insert Position

We conducted an analysis to observe the impact of integrating our dynamic prompt in various depths of Transformer layers. The experimental results, as demonstrated in Figure 5 (a) and (b), indicated that the addition of a prompt to deeper layers resulted in better performance. This can be attributed to the fact that our prompt generation module utilizes patch tokens to perceive the semantic priors of each point cloud, and deeper patch tokens comprise more comprehensive semantic information.

Additionally, we found that applying the prompt to all layers using a prompt module with shared parameters in the "all_layer" setting did not produce satisfactory results. This is due to the fact that the shared prompt module can cause degradation in the semantic prior representation, and using independent parameters for each layer would result in an unacceptable increase in the number of parameters. As a result, we decided to add the prompt to the input of the final layer of the Transformer.

4.3.5 Qualitative analysis of the ability to approximate the transformation $\Phi(\cdot)$ in DA

We analyzed the effectiveness of various tuning strategies for the transformation function $\Phi(\cdot)$ by conducting a qualitative analysis of their fitting ability. The strategies we evaluated included (a) the pre-trained model, (b) VPT-Deep,

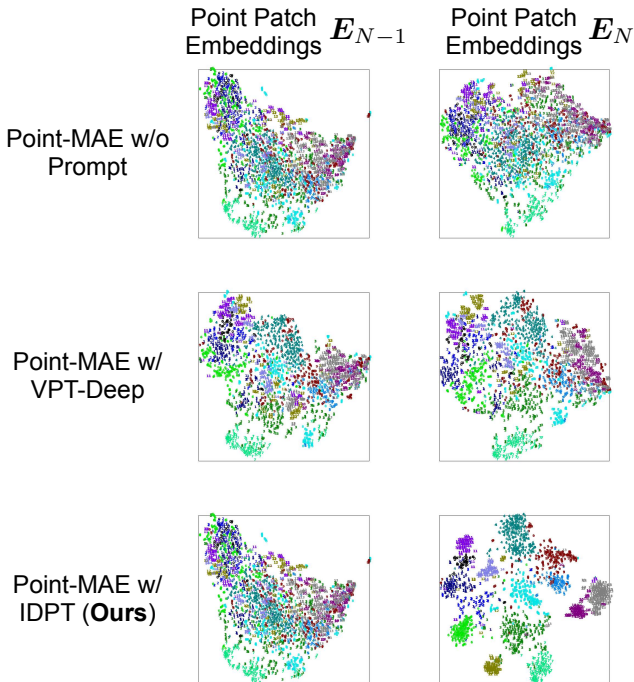


Figure 6. The t-SNE visualization of the point patch features extracted E_{N-1} and E_N from the test sets of ScanObjectNN (PB_T50_RS) using a pre-trained Point-MAE with different tuning strategies. This visualization partly reflects the approximation of the transformation function $\Phi(\cdot)$ by different tuning strategies.

and (c) IDPT. To visualize the input (E_{N-1}) and output (E_N) of all point patches in the N -th layer of the Transformer on ScanObjectNN, we utilized a pre-trained model based on Point-MAE. The results of our visualization are presented in Figure 6, which displays the visualization outcomes of the three tuning strategies.

The performance of different strategies for approximating the function $\Phi(\cdot)$ with the Transformer model varies. The pre-trained model (a) uses the Transformer with fixed parameters and shows the worst performance. VPT-Deep (b), which adds trainable static prompt parameters to all layers' inputs to approximate $\Phi(\cdot)$, resulting in a better input feature distribution E_{N-1} in the N -th layer than (a). However, the output features E_N are still scattered, indicating a poorer $\Phi(\cdot)$ approximate. IDPT takes a different approach by introducing the semantic prior of each instance and adding dynamic prompts to the input space of the N -th layer to approximate $\Phi(\cdot)$. Although the input features E_{N-1} at the N -th layer are as scattered as (a), the output features E_N are tightly clustered for the same category after concatenating E_{N-1} with our prompt through the same network as (a). It indicates that our strategy can effectively align the different distributions and is the best approximate strategy for $\Phi(\cdot)$.

5. Conclusion

In this paper, we examine the introduction of prompt tuning into pre-trained point cloud models as a strategy for reducing the number of parameters needed for downstream tasks. Initially, we adopt visual prompt tuning [23] to point cloud pre-trained models and found that the static prompt tuning cannot work well in real point clouds due to the distribution diversity. To address this issue, we propose an instance-aware dynamic prompt tuning (IDPT) to produce a universal prompt for both synthetic and real point clouds, which is adaptive to instance input. Extensive experimentation validates our IDPT strategy as a universal and effective solution.

A. More Experimental Analysis

A.1. Part segmentation Performance

Methods	#TP (M)	mIoU _c	mIoU _I
PointNet [34]	-	80.39	83.7
PointNet++ [35]	-	81.85	85.1
DGCNN [45]	-	82.33	85.2
Transformer [51]	27.09	83.42	85.1
OcCo [51]	27.09	83.42	85.1
MaskPoint [27]	-	84.60	86.0
Point-BERT [51]	27.09	84.11	85.6
Point-MAE [33]	27.06	84.19	86.1
ACT [11]	27.06	84.66	86.1
Point-MAE w/o prompt	5.24	83.58	85.3
Point-MAE w/ VPT	5.35	83.64	85.4
Point-MAE w/ IDPT	5.69	83.79	85.7

Table 7. Part segmentation results on the ShapeNetPart dataset. The mean IoU across all categories, *i.e.*, mIoU_c (%), and the mean IoU across all instances, *i.e.*, mIoU_I (%) are reported.

For part segmentation, we follow previous work [11, 33] to add prompts to the input of 3-rd, 7-th and 11-th layers and the task head. Since we empirically observed that using a single-layer MLP achieves comparable performance to the three-layer EdgeConv architecture in the segmentation task, we adopt a simple single-layer MLP as the dynamic prompt generation module at each layer to reduce the number of trainable parameters.

According to experimental results in Table 7, our IDPT outperforms the baseline without prompt and static prompting strategy, VPT [23]. It verifies the effectiveness of our dynamic prompting strategy. We can also find prompt tuning strategies still underperform state-of-the-art methods (*e.g.* ACT [11] and Point-MAE [33]) with full finetuning strategies on segmentation. We attribute this gap to the difficulty of fine-grained understanding of point clouds, which makes the downstream adaptation of pre-trained models

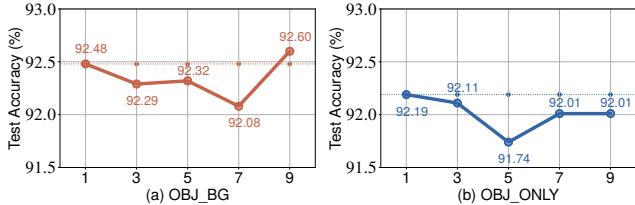


Figure 7. The effect of different numbers of prompts.

with limited tunable parameters a challenging task. Fortunately, our IDPT in the idea of instance-aware dynamics provides an effective solution to mitigate the performance gap. We hope it can provide some inspiration towards better parameter-efficient tuning strategies for fine-grained tasks of point clouds.

A.2. Effect of Prompt Number

In this section, we investigate the impact of prompt numbers in IDPT on classification tasks. By default, we use three layers of EdgeConv [45] and one layer of MLP to extract the semantic information $E_P \in \mathbb{R}^{m \times d}$ from all patches and then use max pooling along the feature dimension to aggregate the semantic information of all patches to generate prompt $P_{N-1} \in \mathbb{R}^{1 \times d}$.

To generate multiple representative prompts, we replace the max pooling operation along the feature dimension with a top- K operation, resulting in K prompts $P'_{N-1} \in \mathbb{R}^{K \times d}$. We then aggregate P'_{N-1} , c_{N-1} , and E_{N-1} and feed them to the last transformer layer f_N .

$$[c_N; P'_N; E_N] = f_N([c_{N-1}; P'_{N-1}; E_{N-1}]). \quad (11)$$

For the classification head, we perform max pooling along the feature dimension of P'_N to obtain $P_N \in \mathbb{R}^{1 \times d}$ as prompt-related input.

We analyze the impact of different prompt numbers on classification tasks. Figure 7 presents the experimental results on two variants of ScanObjectNN. The results indicate that simply increasing the prompt number does not contribute to performance gain. Therefore, we only set a single prompt in IDPT to improve efficiency.

A.3. Inserting Independent Prompt Modules to All Layers

Trainable Parameters Type	#TP (M)	OBJ_BG	OBJ_ONLY
1 PM + Head	1.70	92.48	92.19
12 PM + Head	16.34	92.60	92.22

Table 8. The effect of inserting independent prompt modules to all layers. PM indicates the dynamic prompt generation module.

In Figure 5 of the main paper, we have demonstrated the effect of inserting prompts into multiple layers of the pre-trained point cloud model. Note that we share the prompt

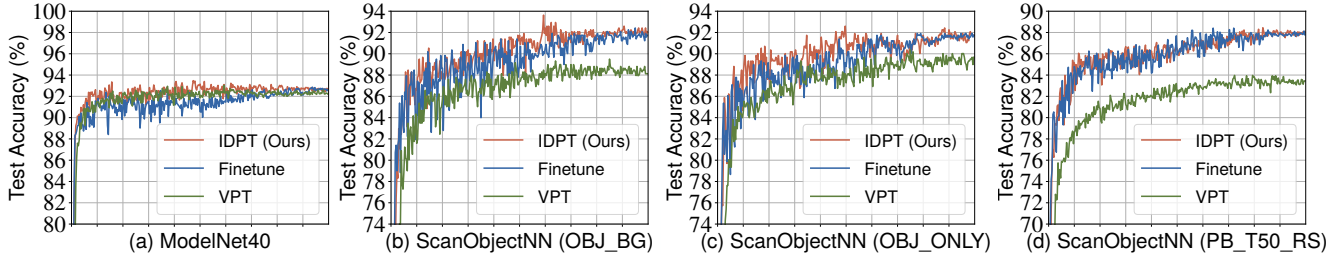


Figure 8. The classification accuracy curves of fine-tuning, VPT, and our IDPT strategy on two datasets.

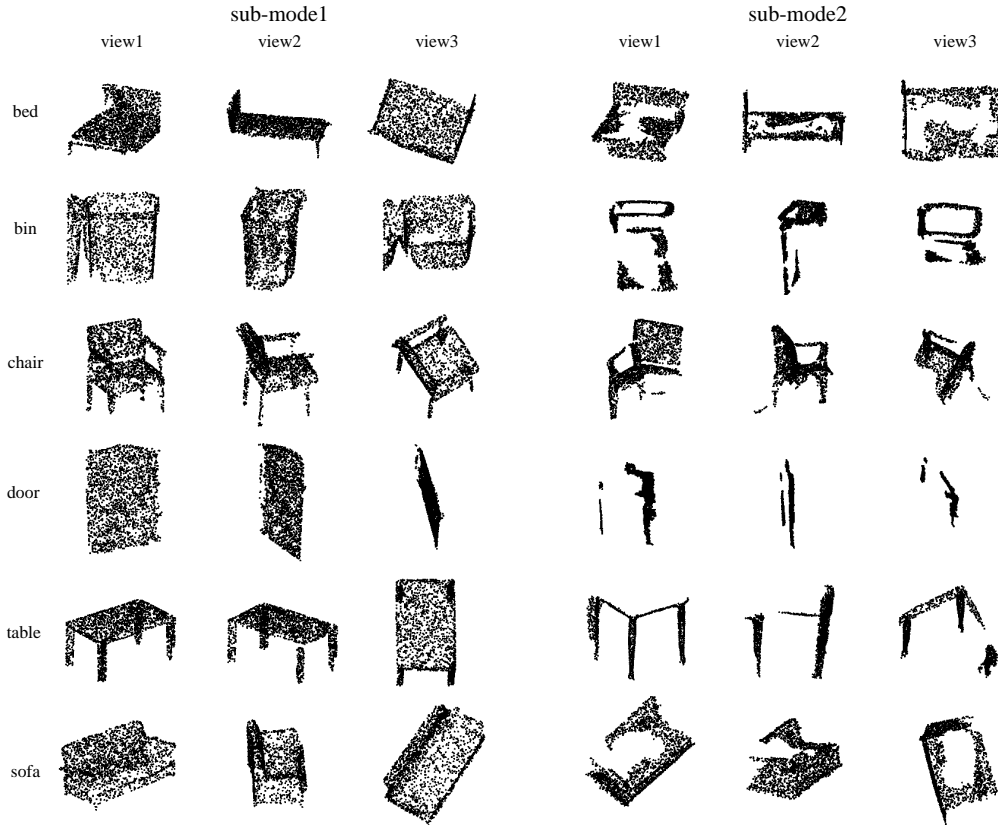


Figure 9. Different sub-modes in each category of ScanObjectNN

generation module among multiple layers in Figure 5 in the spirit of parameter-efficient tuning. Nevertheless, it would be interesting to see the results of inserting independent prompt generation modules into different layers. In particular, here we provide the results of all-layer insertion, as shown in Table 8. The results indicate that incorporating a parameter-independent prompt generation module at every layer only brings marginal improvement with a significant increase of trainable parameters, deviating from the goal of parameter-efficient tuning. Regarding the empirical observations in Figure 5 of the main paper and Table 8, we only insert the dynamic prompt generation module into the last layer of the pre-trained model.

A.4. Convergence of Different Tuning Strategies

In this section, we study how the performances of different tuning strategies change in the whole training process. The accuracy curves of fine-tuning, VPT, and IDPT on two datasets (*i.e.*, ModelNet40 and ScanObjectNN) are illustrated in Figure 8.

As shown in Figure 8, our IDPT strategy achieves significant improvements upon VPT. The performance of IDPT is competitive with fine-tuning on most datasets. Moreover, we can learn that IDPT yields faster convergence by incorporating prior semantic information of instances, revealing the merit of instance-aware dynamics for model adaptation.

A.5. Demonstration of Sub-modes in Real-world Scanned Data

Due to the limitations of scanning techniques, it is prevailing to see various kinds of missing or noisy points in real-world point clouds, corresponding to different sub-modes in the data distribution. Such inconsistent noises will threaten the robustness of prompt-based adaptation, especially for static prompt strategies like VPT [23]. Here we would like to give some point cloud samples to facilitate an intuitive understanding about *how different sub-modes look like*. Specifically, Figure 9 presents different missing types w.r.t. different categories in the ScanObjectNN dataset. We use sub_mode1 and sub_mode2 to differentiate missing types. For each scanned object, we show its projection images from three different viewpoints (*i.e.* view1, view2, and view3) to simulate stereoscopy.

References

- [1] Mohamed Afham, Isuru Dissanayake, Dinithi Dissanayake, Amaya Dharmasiri, Kanchana Thilakarathna, and Ranga Rodrigo. Crosspoint: Self-supervised cross-modal contrastive learning for 3d point cloud understanding. In *Proceedings of the IEEE/CVF Conference on Computer Vision and Pattern Recognition*, pages 9902–9912, 2022. 2
- [2] Armen Aghajanyan, Luke Zettlemoyer, and Sonal Gupta. Intrinsic dimensionality explains the effectiveness of language model fine-tuning. *arXiv preprint arXiv:2012.13255*, 2020. 4
- [3] Alexei Baevski, Wei-Ning Hsu, Qiantong Xu, Arun Babu, Jiatuo Gu, and Michael Auli. Data2vec: A general framework for self-supervised learning in speech, vision and language. *arXiv preprint arXiv:2202.03555*, 2022. 2
- [4] Suzanna Becker and Geoffrey E Hinton. Self-organizing neural network that discovers surfaces in random-dot stereograms. *Nature*, 355(6356):161–163, 1992. 2
- [5] Shai Ben-David, John Blitzer, Koby Crammer, Alex Kulesza, Fernando Pereira, and Jennifer Wortman Vaughan. A theory of learning from different domains. *Machine learning*, 79:151–175, 2010. 4
- [6] Shai Ben-David, John Blitzer, Koby Crammer, and Fernando Pereira. Analysis of representations for domain adaptation. *Advances in neural information processing systems*, 19, 2006. 4
- [7] Tom Brown, Benjamin Mann, Nick Ryder, Melanie Subbiah, Jared D Kaplan, Prafulla Dhariwal, Arvind Neelakantan, Pranav Shyam, Girish Sastry, Amanda Askell, et al. Language models are few-shot learners. *Advances in neural information processing systems*, 33:1877–1901, 2020. 2
- [8] Angel X Chang, Thomas Funkhouser, Leonidas Guibas, Pat Hanrahan, Qixing Huang, Zimo Li, Silvio Savarese, Manolis Savva, Shuran Song, Hao Su, et al. Shapenet: An information-rich 3d model repository. *arXiv preprint arXiv:1512.03012*, 2015. 5
- [9] Ting Chen, Simon Kornblith, Mohammad Norouzi, and Geoffrey Hinton. A simple framework for contrastive learning of visual representations. In *International conference on machine learning*, pages 1597–1607. PMLR, 2020. 2
- [10] Silin Cheng, Xiwu Chen, Xinwei He, Zhe Liu, and Xiang Bai. Pra-net: Point relation-aware network for 3d point cloud analysis. *IEEE Transactions on Image Processing*, 30:4436–4448, 2021. 6
- [11] Runpei Dong, Zekun Qi, Linfeng Zhang, Junbo Zhang, Jianjian Sun, Zheng Ge, Li Yi, and Kaisheng Ma. Autoencoders as cross-modal teachers: Can pretrained 2d image transformers help 3d representation learning? *arXiv preprint arXiv:2212.08320*, 2022. 1, 2, 4, 5, 6, 9
- [12] Alexey Dosovitskiy, Lucas Beyer, Alexander Kolesnikov, Dirk Weissenborn, Xiaohua Zhai, Thomas Unterthiner, Mostafa Dehghani, Matthias Minderer, Georg Heigold, Sylvain Gelly, et al. An image is worth 16x16 words: Transformers for image recognition at scale. *arXiv preprint arXiv:2010.11929*, 2020. 1
- [13] Tianyu Gao, Adam Fisch, and Danqi Chen. Making pre-trained language models better few-shot learners. *arXiv preprint arXiv:2012.15723*, 2020. 2
- [14] Spyros Gidaris, Praveer Singh, and Nikos Komodakis. Unsupervised representation learning by predicting image rotations. *arXiv preprint arXiv:1803.07728*, 2018. 2
- [15] Ankit Goyal, Hei Law, Bowei Liu, Alejandro Newell, and Jia Deng. Revisiting point cloud shape classification with a simple and effective baseline. In *International Conference on Machine Learning*, pages 3809–3820. PMLR, 2021. 6
- [16] Meng-Hao Guo, Jun-Xiong Cai, Zheng-Ning Liu, Tai-Jiang Mu, Ralph R Martin, and Shi-Min Hu. Pct: Point cloud transformer. *Computational Visual Media*, 7(2):187–199, 2021. 1, 6
- [17] Xu Guo and Han Yu. On the domain adaptation and generalization of pretrained language models: A survey. *arXiv preprint arXiv:2211.03154*, 2022. 4
- [18] Abdullah Hamdi, Silvio Giancola, and Bernard Ghanem. Mvtn: Multi-view transformation network for 3d shape recognition. In *Proceedings of the IEEE/CVF International Conference on Computer Vision*, pages 1–11, 2021. 6
- [19] Kaiming He, Xinlei Chen, Saining Xie, Yanghao Li, Piotr Dollár, and Ross Girshick. Masked autoencoders are scalable vision learners. In *Proceedings of the IEEE/CVF Conference on Computer Vision and Pattern Recognition*, pages 16000–16009, 2022. 2
- [20] Neil Houlsby, Andrei Giurgiu, Stanislaw Jastrzebski, Bruna Morrone, Quentin De Laroussilhe, Andrea Gesmundo, Mona Attariyan, and Sylvain Gelly. Parameter-efficient transfer learning for nlp. In *International Conference on Machine Learning*, pages 2790–2799. PMLR, 2019. 7
- [21] Tianyu Huang, Bowen Dong, Yunhan Yang, Xiaoshui Huang, Rynson WH Lau, Wanli Ouyang, and Wangmeng Zuo. Clip2point: Transfer clip to point cloud classification with image-depth pre-training. *arXiv preprint arXiv:2210.01055*, 2022. 1, 2, 6
- [22] Xiaoshui Huang, Sheng Li, Wentao Qu, Tong He, Yifan Zuo, and Wanli Ouyang. Frozen clip model is efficient point cloud backbone. *arXiv preprint arXiv:2212.04098*, 2022. 1, 6

- [23] Menglin Jia, Luming Tang, Bor-Chun Chen, Claire Cardie, Serge Belongie, Bharath Hariharan, and Ser-Nam Lim. Visual prompt tuning. In *Computer Vision—ECCV 2022: 17th European Conference, Tel Aviv, Israel, October 23–27, 2022, Proceedings, Part XXXIII*, pages 709–727. Springer, 2022. [1](#), [2](#), [3](#), [4](#), [7](#), [9](#), [11](#)
- [24] Brian Lester, Rami Al-Rfou, and Noah Constant. The power of scale for parameter-efficient prompt tuning. *arXiv preprint arXiv:2104.08691*, 2021. [2](#)
- [25] Yangyan Li, Rui Bu, Mingchao Sun, Wei Wu, Xinhan Di, and Baoquan Chen. Pointcnn: Convolution on x-transformed points. *Advances in neural information processing systems*, 31, 2018. [1](#), [6](#)
- [26] Kevin Lin, Lijuan Wang, and Zicheng Liu. End-to-end human pose and mesh reconstruction with transformers. In *Proceedings of the IEEE/CVF Conference on Computer Vision and Pattern Recognition*, pages 1954–1963, 2021. [2](#)
- [27] Haotian Liu, Mu Cai, and Yong Jae Lee. Masked discrimination for self-supervised learning on point clouds. In *Computer Vision—ECCV 2022: 17th European Conference, Tel Aviv, Israel, October 23–27, 2022, Proceedings, Part II*, pages 657–675. Springer, 2022. [1](#), [2](#), [6](#), [9](#)
- [28] Pengfei Liu, Weizhe Yuan, Jinlan Fu, Zhengbao Jiang, Hiroaki Hayashi, and Graham Neubig. Pre-train, prompt, and predict: A systematic survey of prompting methods in natural language processing. *ACM Computing Surveys*, 55(9):1–35, 2023. [2](#)
- [29] Xiao Liu, Kaixuan Ji, Yicheng Fu, Zhengxiao Du, Zhilin Yang, and Jie Tang. P-tuning v2: Prompt tuning can be comparable to fine-tuning universally across scales and tasks. *arXiv preprint arXiv:2110.07602*, 2021. [2](#)
- [30] Xiao Liu, Yanan Zheng, Zhengxiao Du, Ming Ding, Yujie Qian, Zhilin Yang, and Jie Tang. Gpt understands, too. *arXiv preprint arXiv:2103.10385*, 2021. [2](#)
- [31] Yongcheng Liu, Bin Fan, Shiming Xiang, and Chunhong Pan. Relation-shape convolutional neural network for point cloud analysis. In *Proceedings of the IEEE/CVF Conference on Computer Vision and Pattern Recognition*, pages 8895–8904, 2019. [6](#)
- [32] Xu Ma, Can Qin, Haoxuan You, Haoxi Ran, and Yun Fu. Rethinking network design and local geometry in point cloud: A simple residual mlp framework. *arXiv preprint arXiv:2202.07123*, 2022. [1](#), [6](#)
- [33] Yatian Pang, Wenxiao Wang, Francis EH Tay, Wei Liu, Yonghong Tian, and Li Yuan. Masked autoencoders for point cloud self-supervised learning. *arXiv preprint arXiv:2203.06604*, 2022. [1](#), [2](#), [3](#), [4](#), [5](#), [6](#), [9](#)
- [34] Charles R Qi, Hao Su, Kaichun Mo, and Leonidas J Guibas. Pointnet: Deep learning on point sets for 3d classification and segmentation. In *Proceedings of the IEEE conference on computer vision and pattern recognition*, pages 652–660, 2017. [1](#), [6](#), [9](#)
- [35] Charles Ruizhongtai Qi, Li Yi, Hao Su, and Leonidas J Guibas. Pointnet++: Deep hierarchical feature learning on point sets in a metric space. *Advances in neural information processing systems*, 30, 2017. [1](#), [6](#), [9](#)
- [36] Shi Qiu, Saeed Anwar, and Nick Barnes. Dense-resolution network for point cloud classification and segmentation. In *Proceedings of the IEEE/CVF Winter Conference on Applications of Computer Vision*, pages 3813–3822, 2021. [6](#)
- [37] Shi Qiu, Saeed Anwar, and Nick Barnes. Geometric back-projection network for point cloud classification. *IEEE Transactions on Multimedia*, 24:1943–1955, 2021. [6](#)
- [38] Alec Radford, Jong Wook Kim, Chris Hallacy, Aditya Ramesh, Gabriel Goh, Sandhini Agarwal, Girish Sastry, Amanda Askell, Pamela Mishkin, Jack Clark, et al. Learning transferable visual models from natural language supervision. In *International conference on machine learning*, pages 8748–8763. PMLR, 2021. [1](#), [2](#)
- [39] Yongming Rao, Wenliang Zhao, Guangyi Chen, Yansong Tang, Zheng Zhu, Guan Huang, Jie Zhou, and Jiwen Lu. Denseclip: Language-guided dense prediction with context-aware prompting. In *Proceedings of the IEEE/CVF Conference on Computer Vision and Pattern Recognition*, pages 18082–18091, 2022. [2](#)
- [40] Maria Tsimpoukelli, Jacob L Menick, Serkan Cabi, SM Eslami, Oriol Vinyals, and Felix Hill. Multimodal few-shot learning with frozen language models. *Advances in Neural Information Processing Systems*, 34:200–212, 2021. [2](#)
- [41] Mikaela Angelina Uy, Quang-Hieu Pham, Binh-Son Hua, Thanh Nguyen, and Sai-Kit Yeung. Revisiting point cloud classification: A new benchmark dataset and classification model on real-world data. In *Proceedings of the IEEE/CVF international conference on computer vision*, pages 1588–1597, 2019. [2](#), [4](#), [5](#), [6](#), [7](#)
- [42] Laurens Van der Maaten and Geoffrey Hinton. Visualizing data using t-sne. *Journal of machine learning research*, 9(11), 2008. [4](#)
- [43] Ashish Vaswani, Noam Shazeer, Niki Parmar, Jakob Uszkoreit, Llion Jones, Aidan N Gomez, Łukasz Kaiser, and Illia Polosukhin. Attention is all you need. *Advances in neural information processing systems*, 30, 2017. [2](#), [6](#)
- [44] Hanchen Wang, Qi Liu, Xiangyu Yue, Joan Lasenby, and Matt J Kusner. Unsupervised point cloud pre-training via occlusion completion. In *Proceedings of the IEEE/CVF international conference on computer vision*, pages 9782–9792, 2021. [6](#)
- [45] Yue Wang, Yongbin Sun, Ziwei Liu, Sanjay E Sarma, Michael M Bronstein, and Justin M Solomon. Dynamic graph cnn for learning on point clouds. *Acm Transactions On Graphics (tog)*, 38(5):1–12, 2019. [1](#), [3](#), [5](#), [6](#), [9](#)
- [46] Ziyi Wang, Xumin Yu, Yongming Rao, Jie Zhou, and Jiwen Lu. P2p: Tuning pre-trained image models for point cloud analysis with point-to-pixel prompting. *arXiv preprint arXiv:2208.02812*, 2022. [1](#), [2](#), [6](#)
- [47] Zhirong Wu, Shuran Song, Aditya Khosla, Fisher Yu, Linguang Zhang, Xiaoou Tang, and Jianxiong Xiao. 3d shapenets: A deep representation for volumetric shapes. In *Proceedings of the IEEE conference on computer vision and pattern recognition*, pages 1912–1920, 2015. [2](#), [4](#), [6](#)
- [48] Zhirong Wu, Yuanjun Xiong, Stella X Yu, and Dahua Lin. Unsupervised feature learning via non-parametric instance discrimination. In *Proceedings of the IEEE conference on computer vision and pattern recognition*, pages 3733–3742, 2018. [2](#)

- [49] Saining Xie, Jiatao Gu, Demi Guo, Charles R Qi, Leonidas Guibas, and Or Litany. Pointcontrast: Unsupervised pre-training for 3d point cloud understanding. In *European conference on computer vision*, pages 574–591. Springer, 2020. [2](#)
- [50] Li Yi, Vladimir G Kim, Duygu Ceylan, I-Chao Shen, Mengyan Yan, Hao Su, Cewu Lu, Qixing Huang, Alla Sheffer, and Leonidas Guibas. A scalable active framework for region annotation in 3d shape collections. *ACM Transactions on Graphics (ToG)*, 35(6):1–12, 2016. [4](#)
- [51] Xumin Yu, Lulu Tang, Yongming Rao, Tiejun Huang, Jie Zhou, and Jiwen Lu. Point-bert: Pre-training 3d point cloud transformers with masked point modeling. In *Proceedings of the IEEE/CVF Conference on Computer Vision and Pattern Recognition*, pages 19313–19322, 2022. [1](#), [2](#), [5](#), [6](#), [9](#)
- [52] Cheng Zhang, Haocheng Wan, Shengqiang Liu, Xinyi Shen, and Zizhao Wu. Pvt: Point-voxel transformer for 3d deep learning. *arXiv preprint arXiv:2108.06076*, 2, 2021. [6](#)
- [53] Renrui Zhang, Ziyu Guo, Wei Zhang, Kunchang Li, Xupeng Miao, Bin Cui, Yu Qiao, Peng Gao, and Hongsheng Li. Pointclip: Point cloud understanding by clip. In *Proceedings of the IEEE/CVF Conference on Computer Vision and Pattern Recognition*, pages 8552–8562, 2022. [1](#), [2](#)
- [54] Yabin Zhang, Jiehong Lin, Ruihuang Li, Kui Jia, and Lei Zhang. Point-dae: Denoising autoencoders for self-supervised point cloud learning. *arXiv preprint arXiv:2211.06841*, 2022. [1](#), [2](#), [6](#)
- [55] Kaiyang Zhou, Jingkang Yang, Chen Change Loy, and Ziwei Liu. Conditional prompt learning for vision-language models. In *Proceedings of the IEEE/CVF Conference on Computer Vision and Pattern Recognition*, pages 16816–16825, 2022. [2](#)
- [56] Kaiyang Zhou, Jingkang Yang, Chen Change Loy, and Ziwei Liu. Learning to prompt for vision-language models. *International Journal of Computer Vision*, 130(9):2337–2348, 2022. [2](#), [3](#)